

# Multivariate time-series modeling with generative neural networks

Marius Hofert<sup>1</sup>, Avinash Prasad<sup>2</sup>, Mu Zhu<sup>3</sup>

2022-05-28

## Abstract

Generative moment matching networks (GMMNs) are introduced as dependence models for the joint innovation distribution of multivariate time series (MTS). Following the popular copula-GARCH approach for modeling dependent MTS data, a framework based on a GMMN-GARCH approach is presented. First, ARMA-GARCH models are utilized to capture the serial dependence within each univariate marginal time series. Second, if the number of marginal time series is large, principal component analysis (PCA) is used as a dimension-reduction step. Last, the remaining cross-sectional dependence is modeled via a GMMN, the main contribution of this work. GMMNs are highly flexible and easy to simulate from, which is a major advantage over the copula-GARCH approach. Applications involving yield curve modeling and the analysis of foreign exchange rate returns demonstrate the utility of the GMMN-GARCH approach, especially in terms of producing better empirical predictive distributions and making better probabilistic forecasts. All results are reproducible with the demo `GMMN_MTS_paper` of the R package `gmn`.

## Keywords

Generative moment matching networks, learning distributions, copulas, probabilistic forecasts, ARMA-GARCH model, yield curves, exchange rate dependence.

## MSC2010

62H99, 65C60, 60E05, 00A72, 65C10, 62M10.

## 1 Introduction

We extend the popular *copula-GARCH approach* (Jondeau and Rockinger 2006; Patton 2006) for modeling multivariate time series (MTS) data by replacing parametric copulas with generative neural networks. Our primary goal is to make probabilistic forecasts by constructing empirical predictive distributions. Quantities we are interested in forecasting include not just the average value but also quantiles, tail probabilities and others at any given time point in the future.

### Copula-GARCH approach

Typically, there are two types of dependence in MTS data: serial dependence within each univariate time series, and cross-sectional dependence between the individual time series. A key feature of the copula-GARCH approach is that it models these two types of dependence separately.

<sup>1</sup>Department of Statistics and Actuarial Science, University of Waterloo, 200 University Avenue West, Waterloo, ON, N2L 3G1, [mariaus.hofert@uwaterloo.ca](mailto:mariaus.hofert@uwaterloo.ca). The author acknowledges support from NSERC (Grant RGPIN-2020-04897).

<sup>2</sup>Department of Statistics and Actuarial Science, University of Waterloo, 200 University Avenue West, Waterloo, ON, N2L 3G1, [a2prasad@uwaterloo.ca](mailto:a2prasad@uwaterloo.ca). The author acknowledges support from NSERC (PGS D Scholarship).

<sup>3</sup>Department of Statistics and Actuarial Science, University of Waterloo, 200 University Avenue West, Waterloo, ON, N2L 3G1, [mu.zhu@uwaterloo.ca](mailto:mu.zhu@uwaterloo.ca). The author acknowledges support from NSERC (RGPIN-2016-03876).

First, for serial dependence within each univariate time series, the copula–GARCH approach uses a class of generalized auto-regressive conditional heteroscedasticity (GARCH) models (Bollerslev 1986). While there is a plethora of literature on univariate time series modeling with a wide range of models that are tailor-made for capturing various types of serial patterns such as seasonality, volatility clustering or regime switching, GARCH-type models are popular choices in the realm of financial econometrics because they are designed to account for various stylized facts (such as volatility clustering) that are often present in financial return series data; see McNeil et al. (2015, Chapter 3).

Second, for cross-sectional dependence between the individual time series, the copula–GARCH approach leverages Sklar’s Theorem (Sklar 1959) to allow the use of any copula to model the joint innovation distribution. This extends various classic approaches (e.g., Bollerslev 1990; Engle 2002; Tse and Tsui 2002) that rely on the multivariate normal distribution to model the cross-sectional dependence, and is the main attraction that makes the copula–GARCH approach a highly flexible modeling approach. For a brief overview of its versatility and popularity in the context of finance and econometrics, see Patton (2012); for the calibration of these models, see Aas (2016), Almeida et al. (2016), as well as Oh and Patton (2017).

## Motivation

While there is a growing collection of copula models to characterize complex dependence structures, most of them are already limited in moderately large dimensions and often do not provide an adequate fit to given data (e.g., Hofert and Oldford 2018). Identifying appropriate copula models, estimating their parameters and, especially, testing their goodness-of-fit and selecting the final model are time-consuming at best. These modeling steps often require sophisticated algorithms but still do not lead to an adequate model among the computationally tractable ones. To address these shortcomings, we propose to replace parametric copula models in the copula–GARCH approach with a generative moment matching network (GMMN). In comparison to parametric copulas, GMMNs can capture a much larger variety of complex dependence structures. We call this alternative modeling approach the *GMMN–GARCH approach*.

For high-dimensional MTS data, we also incorporate principal component analysis (PCA) as an intermediate step to reduce the dimensionality. Thus, our proposed GMMN–GARCH approach consists of the following three components:

- 1) serial dependence modeling — while many possibilities can be considered, here we deliberately do not deviate from the copula–GARCH approach and use marginal ARMA–GARCH models;
- 2) dimension reduction (optional) — several choices are available, but when this step is needed we simply apply PCA; and
- 3) cross-sectional dependence modeling — here, the copula–GARCH approach would choose a parametric copula, but we introduce the use of GMMNs, the main contribution of this paper.

## Organization

In Section 2, we outline our framework for modeling MTS data. In particular, we focus on the novel integration of GMMNs within this framework. In Section 3, we discuss how to make probabilistic forecasts and evaluate the performance of our MTS model. Then in Section 4, we showcase our GMMN-based multivariate time series model in applications to yield curve and exchange rate data. Section 5 provides concluding remarks. All results in this paper can be reproduced with the demo `GMMN_MTS_paper` in the R package `gmn` (version 0.0-3).

## 2 Framework for multivariate time series modeling

Let  $(\mathbf{X}_t)_{t \in \mathbb{Z}}$  denote a  $d$ -dimensional time series of interest, where  $\mathbf{X}_t = (X_{t,1}, \dots, X_{t,d})$ . Furthermore, consider a stretch of  $\tau$  realizations from  $(\mathbf{X}_t)_{t \in \mathbb{Z}}$  denoted by  $\mathbf{X}_1, \dots, \mathbf{X}_\tau$ . For applications in finance, these are often log-returns of  $d$  asset prices (and negative log-returns for applications in risk management); see Section 4 for more details. In this section, we describe in more depth the three modeling components outlined in Section 1 above.

### 2.1 Modeling serial dependence

The *ARMA–GARCH models* in Step 1) are ARMA models with GARCH errors; see McNeil et al. (2015, Section 4.2.3). An ARMA( $p_{1j}, q_{1j}$ )–GARCH( $p_{2j}, q_{2j}$ ) model has the form

$$\begin{aligned} X_{t,j} &= \mu_{t,j} + \sigma_{t,j} Z_{t,j}, \\ \mu_{t,j} &= \mu_j + \sum_{k=1}^{p_{1j}} \phi_{jk} (X_{t-k,j} - \mu_j) + \sum_{l=1}^{q_{1j}} \gamma_{jl} (X_{t-l,j} - \mu_{t-l,j}), \\ \sigma_{t,j}^2 &= \omega_j + \sum_{k=1}^{p_{2j}} \alpha_{jk} (X_{t-k,j} - \mu_{t-k,j})^2 + \sum_{l=1}^{q_{2j}} \beta_{jl} \sigma_{t-l,j}^2, \end{aligned}$$

where, for each component  $j = 1, \dots, d$ , one has  $\mu_j \in \mathbb{R}$ ,  $\omega_j > 0$ , and  $\alpha_{jk}, \beta_{jl} \geq 0$  for all  $k, l$ . Additional conditions on the coefficients  $\phi_{jk}, \gamma_{jl}, \alpha_{jk}$  and  $\beta_{jl}$  are necessary to ensure that the ARMA–GARCH processes are causal and covariance stationary; see, e.g., McNeil et al. (2015, Section 4.1.2–4.2.2) for the details. For each  $j = 1, \dots, d$ , the *innovations*  $Z_{t,j}$  in the definition of the ARMA–GARCH model are independent and identically distributed (iid) random variables with  $\mathbb{E}(Z_{t,j}) = 0$  and  $\text{Var}(Z_{t,j}) = 1$ ; their realizations after fitting marginal ARMA( $p_{1j}, q_{1j}$ )–GARCH( $p_{2j}, q_{2j}$ ) models are known as *standardized residuals* and denoted by  $\hat{Z}_{t,j}$ ,  $t = 1, \dots, \tau$  and  $j = 1, \dots, d$ . In financial time series applications, common choices of innovation distributions include the standard normal, the scaled  $t$  and the skewed  $t$  distribution.

Fitting marginal time series models is typically done by fitting low-order models with likelihood-based methods and selecting the most adequate fit using the AIC/BIC model selection criterion among the candidate models. A popular broad-brush approach is to fit a GARCH(1, 1) model for financial return series — specifically, an ARMA(0, 0)–GARCH(1, 1) model in our context — and continue the modeling based on the standardized residuals  $\hat{Z}_{1,j}, \dots, \hat{Z}_{\tau,j}$ ; see McNeil et al. (2015, Chapter 4) or Hofert, Kojadinovic, et al. (2018, Section 6.2.3). This procedure is also referred to as *deGARCHing*. With the help of model diagnostic tools — for example, plots of the autocorrelation function (ACF) of  $\hat{Z}_{1,j}, \dots, \hat{Z}_{\tau,j}$  and that of their squared values, Ljung–Box tests or an assessment of the innovation distribution through Q–Q plots — one can then assess the adequacy of each marginal time series model. In what follows we use  $\hat{\mu}_{t,j}$  and  $\hat{\sigma}_{t,j}^2$  to denote the estimated conditional mean and variance models for the  $j$ th marginal time series with orders  $\hat{p}_{1j}, \hat{q}_{1j}, \hat{p}_{2j}, \hat{q}_{2j}$  and fitted parameters  $\hat{\phi}_{jk}, \hat{\gamma}_{jl}, \hat{\alpha}_{jk}, \hat{\beta}_{jl}$ .

Having accounted for the marginal serial dependence in this way, the subsequent analysis in our modeling framework will operate on the standardized residuals  $\hat{\mathbf{Z}}_t = (\hat{Z}_{t,1}, \dots, \hat{Z}_{t,d})$ ,  $t = 1, \dots, \tau$ , which are themselves realizations of the innovation random variables,  $\mathbf{Z}_1, \dots, \mathbf{Z}_\tau$ , assumed to be iid in the copula–GARCH approach.

Note that any other adequate marginal time series modeling approach can be applied in our framework as long as the model’s marginal residuals can be considered to be iid realizations from a continuous distribution. Our choice of ARMA–GARCH models here and in what follows is motivated only from the fact that these are the most popular marginal time series models used in practice.

## 2.2 Dimension reduction

Two popular dimension-reduction techniques for multivariate financial time series are factor models and PCA; see McNeil et al. (2015, Chapter 6) and the references therein for a brief summary. An approach that is perhaps less discussed in the financial econometrics literature involves using autoencoder neural networks for dimension reduction in which two separate neural network mappings are learned to and from the lower dimensional space; see Hinton and Salakhutdinov (2006). As dimension reduction is not our main contribution in this work, we simply utilize PCA in what follows.

Note that PCA is often applied to the MTS data  $\mathbf{X}_1, \dots, \mathbf{X}_\tau$  in the literature; see, e.g., Alexander (2000). Apart from reducing the burden of marginal time series modeling, there is no strong reason why PCA should be applied to potentially non-stationary data. If dimension reduction is necessary, we find it statistically more sound to apply PCA to the standardized residuals  $\hat{\mathbf{Z}}_t$  after first accounting for any serial dependence in the marginal time series.

Let  $\hat{\Sigma}$  denote the sample covariance matrix of the standardized residuals  $\hat{\mathbf{Z}}_t, t = 1, \dots, \tau$ . The result from PCA is the matrix  $\hat{\Gamma} \in \mathbb{R}^{d \times d}$  whose columns consist of the eigenvectors of  $\hat{\Sigma}$ , sorted according to decreasing eigenvalues  $\hat{\lambda}_1 \geq \dots \geq \hat{\lambda}_d \geq 0$ . For the purposes of dimension reduction,  $\hat{\mathbf{Z}}_t, t = 1, \dots, \tau$ , are transformed to  $\hat{\mathbf{Y}}_t = \hat{\Gamma}_{:,1:k}^\top \hat{\mathbf{Z}}_t$ , where  $\hat{\Gamma}_{:,1:k} \in \mathbb{R}^{d \times k}$  represent the first  $k$  columns of  $\hat{\Gamma}$  for some  $1 \leq k < d$ . As a result, the sample covariance matrix of  $\mathbf{Y}_t$  is (approximately) diagonal, and the components of  $\mathbf{Y}_t$  are (approximately) uncorrelated. The  $j$ th component series  $Y_{1,j}, \dots, Y_{\tau,j}$ , forms realizations of the  $j$ th principal component, and the first  $k$  principal component series account for  $\sum_{j=1}^k \hat{\lambda}_j / \sum_{j=1}^d \hat{\lambda}_j$  of the total variance.

As dimension reduction is an optional component in our modeling framework, the next step involves dependence modeling of either the standardized residuals  $\hat{\mathbf{Z}}_1, \dots, \hat{\mathbf{Z}}_\tau$  directly or their principal components  $\hat{\mathbf{Y}}_1, \dots, \hat{\mathbf{Y}}_\tau$ . To unify the notation for both cases, we define a  $d^*$ -dimensional time series  $\hat{\mathbf{Y}}_t = \hat{\Upsilon}^\top \hat{\mathbf{Z}}_t$ , where  $\hat{\Upsilon} = \hat{\Gamma}_{:,1:k}$  if dimension reduction is employed and  $\hat{\Upsilon} = I_d$  (the identity matrix in  $\mathbb{R}^{d \times d}$ ) otherwise; consequently,  $d^* = k$  in the former case and  $d^* = d$  in the latter. Furthermore, we treat  $\hat{\mathbf{Y}}_1, \dots, \hat{\mathbf{Y}}_\tau$  as realizations from  $\mathbf{Y}_t$  and so naturally,  $\mathbf{Y}_t = \Upsilon^\top \mathbf{Z}_t$  with  $\Upsilon = \Gamma_{:,1:k}$  if dimension reduction is used and  $\Upsilon = I_d$  otherwise.

## 2.3 Modeling cross-sectional dependence

The final task in our framework involves the modeling of the iid series  $\mathbf{Y}_1, \dots, \mathbf{Y}_\tau$ . To account for cross-sectional dependence, we model the joint distribution function  $H$  of  $\mathbf{Y}_t$  using Sklar's Theorem as

$$H(\mathbf{y}) = C(F_1(y_1), \dots, F_{d^*}(y_{d^*})), \quad \mathbf{y} \in \mathbb{R}^{d^*},$$

where  $F_j, j = 1, \dots, d^*$ , are the margins of  $H$  and  $C : [0, 1]^{d^*} \rightarrow [0, 1]$  is the copula of  $(Y_{t,1}, \dots, Y_{t,d^*})$  for each  $t$ .

Following a classical copula modeling approach, one first builds the *pseudo-observations*  $\hat{U}_{t,j} = R_{t,j}/(\tau + 1)$ ,  $t = 1, \dots, \tau, j = 1, \dots, d^*$ , where  $R_{t,j}$  denotes the rank of  $\hat{Y}_{t,j}$  among  $\hat{Y}_{1,j}, \dots, \hat{Y}_{\tau,j}$ . The pseudo-observations are viewed as realizations from  $C$  based on which one would fit candidate copula models; see, e.g., McNeil et al. (2015, Section 7.5.1) or Hofert, Kojadinovic, et al. (2018, Section 4.1.2). Note that by considering the non-parametric pseudo-observations (even in the case when we do not apply a dimension reduction technique and thus know the (fitted) marginal innovation distributions), we reduce the risk of a misspecified margin affecting the estimation of the copula  $C$ ; see Genest and Segers (2010) for a theoretical justification of this approach. Therefore, going forward, we will use the pseudo-observations  $\hat{\mathbf{U}}_t = (\hat{U}_{t,1}, \dots, \hat{U}_{t,d^*})$ ,  $t = 1, \dots, \tau$ , to model the cross-sectional dependence structure of  $\hat{\mathbf{Y}}_t$ .

### 2.3.1 Parametric copulas

A traditional approach for modeling the cross-sectional dependence described by  $\hat{U}_1, \dots, \hat{U}_\tau$  involves the fitting of parametric copula models, their goodness-of-fit assessment and finally, model selection. There are numerous families of copula models to consider depending on prominent features of the dependence structure present in  $\hat{U}_t$  such as (a)symmetries or a concentration of points in the lower/upper tail of the joint distribution (or pairs of such) which hints at an adequate model possessing tail dependence.

A problem with this approach is that it is often hard to find an adequate copula model for given real-life data, especially in higher dimensions where typically some pairwise dependencies contradict the corresponding model-implied marginal copulas; see, e.g., Hofert and Oldford (2018). Another problem is that certain copula models are computationally expensive to fit and test for goodness-of-fit. In Section 4, we investigate whether (the much more flexible) GMMNs can outperform prominent elliptical and Archimedean copulas in the context of our framework. In what follows we thus shall denote by  $\hat{C}_{\text{PM}}$  a (generic) parametric copula model fitted to the pseudo-observations  $\hat{U}_1, \dots, \hat{U}_\tau$ .

### 2.3.2 GMMNs

We propose to utilize generative neural networks (in particular, GMMNs) for modeling the cross-sectional dependence structure of the pseudo-observations  $\hat{U}_1, \dots, \hat{U}_\tau$ . In our framework, a generative neural network  $f_{\hat{\theta}}$  with fitted parameter vector  $\hat{\theta}$  is used as an estimator for the distribution of the pseudo-observations. Let  $\hat{C}_{\text{NN}}$  denote the empirical copula based on a sample generated from a trained GMMN  $f_{\hat{\theta}}$ .

GMMNs, also known as Maximum Mean Discrepancy (MMD) nets, were introduced simultaneously by Li et al. (2015) and Dziugaite et al. (2015). A GMMN  $f_{\theta}$  utilizes a kernel maximum mean discrepancy statistic as the *loss function* to learn the distribution of the pseudo-observations. Conceptually,  $f_{\theta}$  can be thought of as a parametric map from a random vector  $\mathbf{V}_t = (V_{t,1}, \dots, V_{t,p})$  with (known) *prior distribution*  $F_{\mathbf{V}}$  to  $\hat{U}_t = (\hat{U}_{t,1}, \dots, \hat{U}_{t,d^*})$ . As is standard in the literature, we assume that  $V_{t,1}, \dots, V_{t,p}$  are iid. Typical choices of  $F_{\mathbf{V}}$  are  $U(0, 1)$  or  $N(0, 1)$ ; we utilize the latter. Based on the fitted GMMN  $f_{\hat{\theta}} : \mathbb{R}^p \rightarrow [0, 1]^{d^*}$  we can then generate samples with copula  $\hat{C}_{\text{NN}}$  as an approximation to the target copula  $C$  of  $\hat{U}_t$ . As demonstrated in Hofert, Prasad, et al. (2018), GMMNs provide a flexible class of models capable of learning a variety of complex dependence structures.

Next, we briefly discuss three key aspects when applying GMMNs: the architecture of the neural network  $f_{\theta}$ , the loss function and the training procedure for the estimation of  $\theta$ .

### Feedforward neural networks

We now introduce the neural networks we work with in this paper. The *feedforward neural network* (also known as the multi-layer perceptron) is the quintessential deep neural network, which we simply refer to as *neural network (NN)* in what follows. Let  $L$  be the number of hidden layers in the NN and, for each  $l = 0, \dots, L + 1$ , let  $d_l$  be the dimension of layer  $l$ , that is the number of neurons in layer  $l$ . Layer  $l = 0$  refers to the *input layer* which consists of the input  $\mathbf{v}_t \in \mathbb{R}^p$  for  $d_0 = p$ , and layer  $l = L + 1$  refers to the *output layer* which consists of the output  $\mathbf{u}_t \in [0, 1]^{d^*}$  for  $d_{L+1} = d^*$ . The *hidden layers*  $l = 1, \dots, L + 1$  can be described in terms of the output  $\mathbf{a}_{l-1} \in \mathbb{R}^{d_{l-1}}$  of layer  $l - 1$  via

$$\begin{aligned} \mathbf{a}_0 &= \mathbf{v}_t \in \mathbb{R}^{d_0}, \\ \mathbf{a}_l &= f_l(\mathbf{a}_{l-1}) = \phi_l(W_l \mathbf{a}_{l-1} + \mathbf{b}_l) \in \mathbb{R}^{d_l}, \quad l = 1, \dots, L + 1, \\ \mathbf{u}_t &= \mathbf{a}_{L+1} \in \mathbb{R}^{d_{L+1}}, \end{aligned}$$

## 2 Framework for multivariate time series modeling

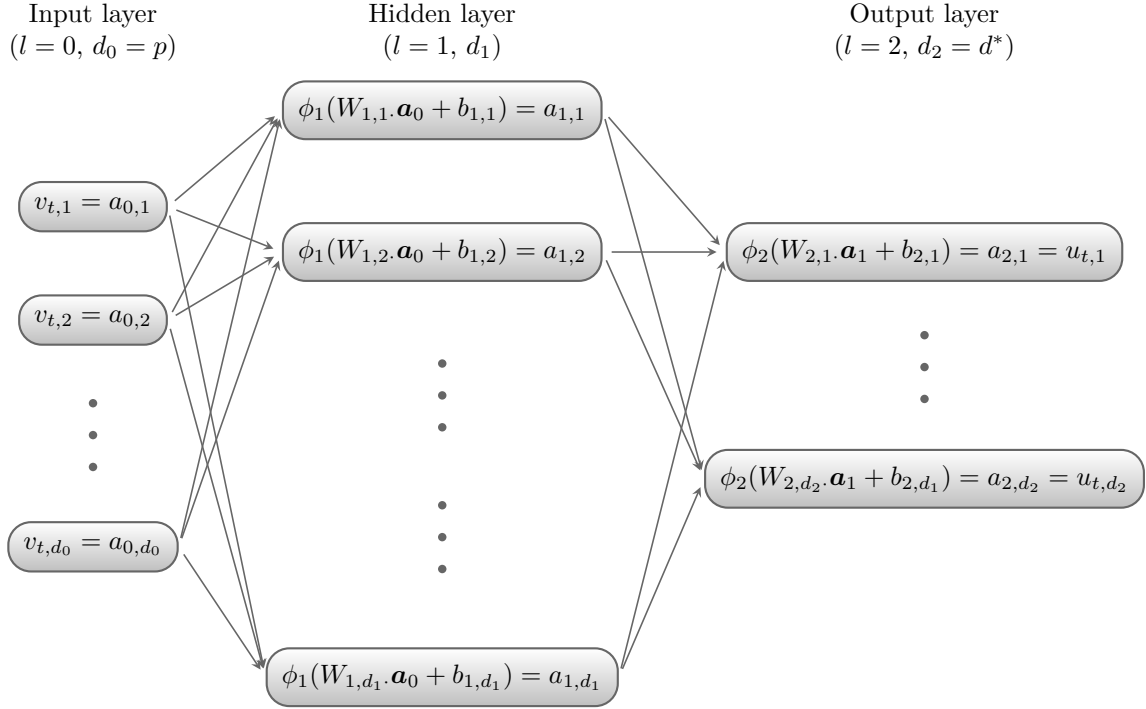


**Figure 1** Structure of a NN with input  $\mathbf{v}_t = (v_{t,1}, \dots, v_{t,d_0})$ ,  $L = 1$  hidden layer with output  $\mathbf{a}_1 = f_1(\mathbf{a}_0) = \phi_1(W_1 \mathbf{a}_0 + \mathbf{b}_1)$  and output layer with output  $\mathbf{u}_t = \mathbf{a}_2 = f_2(\mathbf{a}_1) = \phi_2(W_2 \mathbf{a}_1 + \mathbf{b}_2)$ ; note that,  $W_{l,j}$  denotes the  $j$ th row of  $W_l$  and  $b_{l,j}$  the  $j$ th element of  $\mathbf{b}_l$ .

with *weight matrices*  $W_l \in \mathbb{R}^{d_l \times d_{l-1}}$ , *bias vectors*  $\mathbf{b}_l \in \mathbb{R}^{d_l}$  and *activation functions*  $\phi_l$ ; the latter are understood to be applied componentwise for vector inputs. Some commonly used activation functions include the *sigmoid* activation function  $\phi_l(x) = 1/(1 + e^x)$  and the *rectified linear unit (ReLU)* activation function  $\phi_l(x) = \max\{0, x\}$ . The NN  $f_\theta : \mathbb{R}^p \leftarrow [0, 1]^{d^*}$  can then be written as the composition

$$f_\theta = f_{L+1} \circ f_L \circ \dots \circ f_2 \circ f_1,$$

with its flattened parameter vector  $\theta = (W_1, \dots, W_{L+1}, \mathbf{b}_1, \dots, \mathbf{b}_{L+1})$ . Figure 1 visualizes this construction and the notation we use. GMMNs are such type of NNs which, for training (i.e., the fitting of  $\theta$ ), utilize a specific loss function introduced next.

### Loss function

To learn  $f_\theta$ , we work with  $\tau$  training data points consisting of the pseudo-observations  $\hat{\mathbf{U}}_1, \dots, \hat{\mathbf{U}}_\tau$ . Given an input sample  $\mathbf{V}_1, \dots, \mathbf{V}_{n_{\text{gen}}}$  from the prior distribution  $F_{\mathbf{V}}$ , the GMMN generates an output sample  $\mathbf{U}_1, \dots, \mathbf{U}_{n_{\text{gen}}}$ , where  $\mathbf{U}_t = f_\theta(\mathbf{V}_t)$ ,  $t = 1, \dots, n_{\text{gen}}$ . In selecting an appropriate loss function, we are naturally interested in measuring whether the two samples  $\hat{U} = (\hat{\mathbf{U}}_1^\top, \dots, \hat{\mathbf{U}}_\tau^\top)^\top \in [0, 1]^{\tau \times d^*}$  and  $U = (\mathbf{U}_1^\top, \dots, \mathbf{U}_{n_{\text{gen}}}^\top)^\top \in [0, 1]^{n_{\text{gen}} \times d^*}$  can be deemed to come from the same distribution.

To do so, GMMNs use the *maximum mean discrepancy (MMD)* as loss function, which was introduced as a two-sample test statistic by Gretton et al. (2007). For a given embedding function  $\varphi : \mathbb{R}^{d^*} \mapsto \mathbb{R}^{d'}$ , the MMD measures the distance between two sample statistics,  $(1/\tau) \sum_{t=1}^\tau \varphi(\hat{\mathbf{U}}_{t_1})$  and

$(1/n_{\text{gen}}) \sum_{t_2=1}^{n_{\text{gen}}} \varphi(\mathbf{U}_{t_2})$ , in the embedded space  $\mathbb{R}^d$  via

$$\begin{aligned} & \text{MMD}(\hat{U}, U) \\ &= \left\| \frac{1}{\tau} \sum_{t_1=1}^{\tau} \varphi(\hat{\mathbf{U}}_{t_1}) - \frac{1}{n_{\text{gen}}} \sum_{t_2=1}^{n_{\text{gen}}} \varphi(\mathbf{U}_{t_2}) \right\|_2 \\ &= \left( \frac{1}{\tau^2} \sum_{t_1=1}^{\tau} \sum_{t_2=1}^{\tau} \varphi(\hat{\mathbf{U}}_{t_1})^\top \varphi(\hat{\mathbf{U}}_{t_2}) - \frac{2}{\tau n_{\text{gen}}} \sum_{t_1=1}^{\tau} \sum_{t_2=1}^{n_{\text{gen}}} \varphi(\hat{\mathbf{U}}_{t_1})^\top \varphi(\mathbf{U}_{t_2}) + \frac{1}{n_{\text{gen}}^2} \sum_{t_1=1}^{n_{\text{gen}}} \sum_{t_2=1}^{n_{\text{gen}}} \varphi(\mathbf{U}_{t_1})^\top \varphi(\mathbf{U}_{t_2}) \right)^{1/2}. \end{aligned}$$

If we can choose  $\varphi(\cdot)$  to be a kind of ‘‘distributional embedding’’, for example, in the sense that the two statistics —  $(1/\tau) \sum_{t_1=1}^{\tau} \varphi(\hat{\mathbf{U}}_{t_1})$  and  $(1/n_{\text{gen}}) \sum_{t_2=1}^{n_{\text{gen}}} \varphi(\mathbf{U}_{t_2})$  — contain all empirical moments of  $\hat{U}$  and  $U$ , respectively, then the MMD criterion can be used as a proxy for measuring whether the two samples have the same distribution.

Amazingly, such an embedding exists. By the so-called ‘‘kernel trick’’, known as early as Mercer (1909) but not widely until support vector machines became popular almost a century later, the inner product  $\varphi(\hat{\mathbf{u}}_t)^\top \varphi(\mathbf{u}_t)$  can be computed in a reproducing kernel Hilbert space by  $K(\hat{\mathbf{u}}_t, \mathbf{u}_t)$ , where  $K(\cdot, \cdot) : \mathbb{R}^{d^*} \times \mathbb{R}^{d^*} \mapsto \mathbb{R}$  denotes a kernel similarity function. Hence, for a given kernel function  $K(\cdot, \cdot)$ , the MMD statistic above is equivalent to

$$\text{MMD}(\hat{U}, U; K) = \left( \frac{1}{\tau^2} \sum_{t_1=1}^{\tau} \sum_{t_2=1}^{\tau} K(\hat{\mathbf{U}}_{t_1}, \hat{\mathbf{U}}_{t_2}) - \frac{2}{\tau n_{\text{gen}}} \sum_{t_1=1}^{\tau} \sum_{t_2=1}^{n_{\text{gen}}} K(\hat{\mathbf{U}}_{t_1}, \mathbf{U}_{t_2}) + \frac{1}{n_{\text{gen}}^2} \sum_{t_1=1}^{n_{\text{gen}}} \sum_{t_2=1}^{n_{\text{gen}}} K(\mathbf{U}_{t_1}, \mathbf{U}_{t_2}) \right)^{1/2}. \quad (1)$$

If  $K(\cdot, \cdot)$  is chosen to be a so-called universal kernel function, such as a Gaussian or Laplace kernel, then the associated implicit embedding  $\varphi : \mathbb{R}^{d^*} \mapsto \mathbb{R}^\infty$  is indeed a ‘‘distributional embedding’’ in the sense described above, and one can show that the MMD converges in probability to 0 for  $\tau, n_{\text{gen}} \rightarrow \infty$  if and only if  $\hat{C}_{\text{NN}} = C$  (Gretton et al. 2007; Gretton et al. 2012).

As suggested by Li et al. (2015), we opt to work with a mixture of Gaussian kernels (rather than a single Gaussian kernel) with different bandwidth parameters,

$$K(\hat{\mathbf{u}}_t, \mathbf{u}_t) = \sum_{i=1}^{n_{\text{krn}}} K(\hat{\mathbf{u}}_t, \mathbf{u}_t; \sigma_i), \quad (2)$$

where  $n_{\text{krn}}$  denotes the number of mixture components and  $K(\hat{\mathbf{u}}_t, \mathbf{u}_t; \sigma) = \exp(-\|\hat{\mathbf{u}}_t - \mathbf{u}_t\|_2^2 / (2\sigma^2))$  is the Gaussian kernel with bandwidth parameter  $\sigma > 0$ .

Thus, to train the GMMN  $f_\theta$ , we perform the optimization

$$\min_{\theta} \text{MMD}(\hat{U}, (f_\theta(V); K_{\text{trn}}),$$

where  $V = (\mathbf{V}_1^\top, \dots, \mathbf{V}_{n_{\text{gen}}}^\top)^\top \in [0, 1]^{n_{\text{gen}} \times p}$ , the NN transform  $f_\theta$  is understood to be applied row-wise, and  $K_{\text{trn}}$  represents the selected mixture of Gaussian kernels used to train the GMMN. The specific choice of the number of mixture components  $n_{\text{krn}}$  and the bandwidth parameters  $\sigma_i, i = 1, \dots, n_{\text{krn}}$  that characterize  $K_{\text{trn}}$  will be provided in Section 4.

## Training GMMNs

We now discuss how we can train the GMMN  $f_\theta$ , that is, how we can estimate the parameter vector  $\theta$ . For the sake of convenience, we always simply set  $n_{\text{gen}} = \tau$  while training the GMMN. (However, after training we can still generate an arbitrary number of samples from  $f_{\hat{\theta}}$ .)

Directly optimizing the MMD loss function in (1), also known as batch optimization, would involve all  $\binom{\tau}{2}$  pairs of observations which is memory-prohibitive even for moderately large  $\tau$ . Hence, we adopt a mini-batch optimization procedure, where we partition the training dataset into *batches* of size  $n_{\text{bat}}$  and use the batches sequentially to update  $\boldsymbol{\theta}$ . After all the training data are exhausted, i.e., roughly  $(\tau/n_{\text{bat}})$ -many gradient steps, one epoch of the training of the GMMN is completed. Batch optimization results as a special case of this mini-batch optimization procedure when we set  $n_{\text{bat}} = \tau$ ; it can be used with relatively small datasets. To update the parameter vector  $\boldsymbol{\theta}$ , we utilize the Adam optimizer of Kingma and Ba (2014) which uses a “memory-sticking gradient” procedure — a weighted combination of the current gradient and past gradients from earlier iterations. The trade-off in utilizing mini-batches, particularly with a smaller batch size  $n_{\text{bat}}$ , is that it uses only a partial MMD loss function when computing each gradient step in the optimization.

Algorithm 2.1 summarizes the training of the GMMN  $f_{\boldsymbol{\theta}}$  with a mini-batch optimization procedure.

### Algorithm 2.1 (Training GMMNs)

- 1) Fix the number  $n_{\text{epo}}$  of epochs and the sample size per batch (the so-called *batch size*)  $1 \leq n_{\text{bat}} \leq \tau$ , where  $n_{\text{bat}}$  is assumed to divide  $\tau$ . Initialize the epoch counter  $k = 0$  and the GMMN’s parameter vector  $\boldsymbol{\theta} = \boldsymbol{\theta}^{(0)}$ ; we follow Glorot and Bengio (2010) and initialize the components of  $\boldsymbol{\theta}^{(0)}$  as  $W_l \sim \text{U}(-\sqrt{6/(d_l + d_{l-1})}, \sqrt{6/(d_l + d_{l-1})})^{d_l \times d_{l-1}}$  and  $\mathbf{b}_l = \mathbf{0}$  for  $l = 1, \dots, L + 1$ .
- 2) Initialize the vectors  $\mathbf{m}_1^{(0)} = \mathbf{0}$  and  $\mathbf{m}_2^{(0)} = \mathbf{0}$ , where  $\mathbf{m}_1^{(0)}$  and  $\mathbf{m}_2^{(0)}$  have the same dimension as the parameter vector  $\boldsymbol{\theta}$ . Following Kingma and Ba (2014), we fix the exponential decay rates  $\beta_1 = 0.9$  and  $\beta_2 = 0.999$ , the step size  $\alpha = 0.001$  and the smoothing constant  $\varepsilon = 10^{-8}$ .
- 3) For epoch  $k = 1, \dots, n_{\text{epo}}$ , do:
  - 3.1) Randomly partition the training sample  $\hat{U}_1, \dots, \hat{U}_\tau$  and the prior distribution sample  $\mathbf{V}_1, \dots, \mathbf{V}_\tau$  into corresponding  $\tau/n_{\text{bat}}$  non-overlapping batches  $\hat{U}_1^{(b)}, \dots, \hat{U}_{n_{\text{bat}}}^{(b)}$  and  $\mathbf{V}_1^{(b)}, \dots, \mathbf{V}_{n_{\text{bat}}}^{(b)}$ ,  $b = 1, \dots, \tau/n_{\text{bat}}$ , of size  $n_{\text{bat}}$  each.
  - 3.2) For batch  $b = 1, \dots, \tau/n_{\text{bat}}$ , let  $r = b + (k - 1)\tau/n_{\text{bat}}$  and do:
    - 3.2.1) Compute the GMMN output  $\mathbf{U}_s^{(b)} = f_{\boldsymbol{\theta}^{(r-1)}}(\mathbf{V}_s^{(b)})$ ,  $s = 1, \dots, n_{\text{bat}}$ .
    - 3.2.2) Compute the gradient  $\nabla^{(r)} = \frac{\partial}{\partial \boldsymbol{\theta}} \text{MMD}(\hat{U}^{(b)}, U^{(b)}; K_{\text{trn}})$  from the samples  $\hat{U}^{(b)} = (\hat{U}_1^{(b)\top}, \dots, \hat{U}_{n_{\text{bat}}}^{(b)\top})^\top$  and  $U^{(b)} = (\mathbf{U}_1^{(b)\top}, \dots, \mathbf{U}_{n_{\text{bat}}}^{(b)\top})^\top$  via automatic differentiation.
    - 3.2.3) Update  $\mathbf{m}_1^{(r)} = \beta_1 \mathbf{m}_1^{(r-1)} + (1 - \beta_1) \nabla^{(r)}$  and compute the bias corrected version  $\tilde{\mathbf{m}}_1^{(r)} = \mathbf{m}_1^{(r)} / (1 - \beta_1^r)$ .
    - 3.2.4) Update  $\mathbf{m}_2^{(r)} = \beta_2 \mathbf{m}_2^{(r-1)} + (1 - \beta_2) (\nabla^{(r)})^2$ , where all operations are understood to be applied componentwise, and compute the bias corrected version  $\tilde{\mathbf{m}}_2^{(r)} = \mathbf{m}_2^{(r)} / (1 - \beta_2^r)$ .
    - 3.2.5) Update the parameter vector  $\boldsymbol{\theta}^{(r)} = \boldsymbol{\theta}^{(r-1)} - \alpha \tilde{\mathbf{m}}_1^{(r)} / (\sqrt{\tilde{\mathbf{m}}_2^{(r)}} + \varepsilon)$ , where all operations are understood to be applied componentwise.
- 4) Return  $\hat{\boldsymbol{\theta}} = \boldsymbol{\theta}^{(n_{\text{epo}}(\tau/n_{\text{bat}}))}$ ; the fitted GMMN is then  $f_{\hat{\boldsymbol{\theta}}}$ .

## 3 Probabilistic forecasts and out-of-sample assessments

We now describe how to make rolling probabilistic forecasts from our estimated MTS model by simulating multiple sample paths forward and constructing *empirical predictive distributions* at each



time point. Furthermore, we address how to assess these forecasts with out-of-sample test data. Specifically, we consider a *test period* consisting of time points  $\tau + 1, \tau + 2, \dots, T$ .

### 3.1 Rolling probabilistic forecasts

Let  $h \in \{1, \dots, T - \tau\}$  denote the simulation horizon. For every  $t = \tau, \dots, T - h$ , once all realizations up to and including time  $t$  — namely,  $(\mathbf{X}_s)_{s \leq t}$  — become available, we can simulate  $n_{\text{pth}}$ -many  $h$ -step ahead sample paths conditional on this past information  $\mathcal{F}_t = \sigma(\{\mathbf{X}_s : s \leq t\})$ . Let

$$\hat{X}_{n_{\text{pth}}, h | \mathcal{F}_t} = \{\hat{\mathbf{X}}_{t+1}^{(i)}, \hat{\mathbf{X}}_{t+2}^{(i)}, \dots, \hat{\mathbf{X}}_{t+h}^{(i)} | \mathcal{F}_t\}_{i=1}^{n_{\text{pth}}}$$

denote such sample paths, encoding an *empirical predictive distribution* at each time point  $t + 1, t + 2, \dots, t + h$ , from which various probabilistic forecasts can be made — for example, we can forecast  $\mathbb{P}(\mathbf{X}_{t+2} > x)$  by  $(1/n_{\text{pth}}) \sum_{i=1}^{n_{\text{pth}}} I(\hat{\mathbf{X}}_{t+2}^{(i)} > x)$ .

Figure 2 provides a schematic illustration of what time periods are used respectively for training and testing, as well as how rolling probabilistic forecasts are made as we move forward step by step in time. In particular, we use the realizations  $\mathbf{X}_1, \dots, \mathbf{X}_\tau$  to train our MTS model and the realizations  $\mathbf{X}_{\tau+1}, \dots, \mathbf{X}_T$  to evaluate the rolling probabilistic forecasts made from our trained MTS model. At each particular time point  $t = \tau, \dots, T - h$ , we use all available realizations up to and including time  $t$ , i.e.,  $\mathcal{F}_t$ , to construct  $h$ -step ahead probabilistic forecasts  $\hat{X}_{n_{\text{pth}}, h | \mathcal{F}_t}$ , but we do not re-fit the MTS model itself.

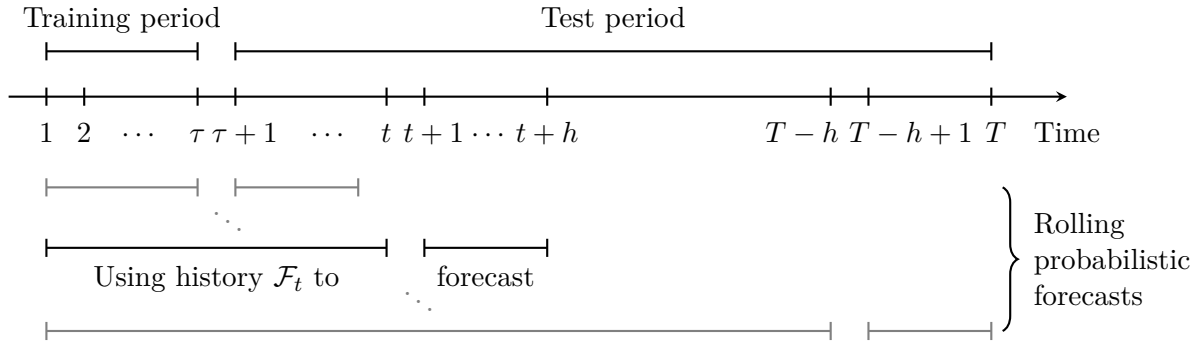


**Figure 2** Time periods used for training, testing and the rolling probabilistic forecasts. At each time point  $t = \tau, \dots, T - h$ , the available history  $\mathcal{F}_t$  is used to make an  $h$ -step ahead probabilistic forecast  $\hat{X}_{n_{\text{pth}}, h | \mathcal{F}_t}$ .

A key component for simulating the paths is the generation of samples from the estimated dependence model. For fitted parametric copulas  $\hat{C}_{\text{PM}}$ , one typically uses a model-specific stochastic representation to sample  $\mathbf{U}_t$ ; see, e.g., Hofert, Kojadinovic, et al. (2018, Chapter 3). Sampling from the fitted GMMN  $f_{\hat{\theta}}$  (with corresponding empirical copula  $\hat{C}_{\text{NN}}$ ) can be done as follows.

#### Algorithm 3.1 (GMMN sampling)

- 1) Fix the number  $n_{\text{gen}}$  of samples to generate from  $\hat{C}_{\text{NN}}$ .
- 2) Draw  $\mathbf{V}_1, \dots, \mathbf{V}_{n_{\text{gen}}} \stackrel{\text{ind.}}{\sim} F_{\mathbf{V}}$  from the prior distribution.
- 3) Return the pseudo-observations of  $\mathbf{U}_s = f_{\hat{\theta}}(\mathbf{V}_s)$ ,  $s = 1, \dots, n_{\text{gen}}$ .

At any particular time point  $t = \tau, \dots, T - h$ , we can now utilize Algorithm 3.1 along with the fitted marginal time series models in our framework in order to simulate paths  $\hat{X}_{n_{\text{pth}},h|\mathcal{F}_t}$  with a fixed horizon  $h$ , as outlined in Algorithm 3.2.

**Algorithm 3.2 (Rolling probabilistic forecasts from a GMMN–GARCH model without re-fitting)**

- 1) Fix the number of sample paths  $n_{\text{pth}}$  and the simulation horizon  $h$ .
- 2) For  $t = \tau, \dots, T - h$  do:
  - 2.1) Generate  $\mathbf{U}_s^{(i)}$ ,  $i = 1, \dots, n_{\text{pth}}$ ,  $s = t + 1, \dots, t + h$ , from the fitted GMMN  $\hat{C}_{\text{NN}}$  via Algorithm 3.1.
  - 2.2) For every  $\mathbf{U}_s^{(i)}$  in Step 2.1), construct  $\mathbf{Y}_s^{(i)} = (\hat{F}_1^{-1}(U_{s,1}^{(i)}), \dots, \hat{F}_{d^*}^{-1}(U_{s,d^*}^{(i)}))$ . If no dimension reduction is utilized,  $\hat{F}_j^{-1}$ ,  $j = 1, \dots, d^*$ , are the quantile functions of the fitted parametric innovation distributions selected as part of the ARMA–GARCH model setup; otherwise, they are the empirical quantile functions of  $\hat{Y}_{1,j}, \dots, \hat{Y}_{\tau,j}$ ,  $j = 1, \dots, d^*$ .
  - 2.3) For every  $\mathbf{Y}_s^{(i)}$  in Step 2.2), construct samples from the fitted innovation distributions via the transform  $\mathbf{Z}_s^{(i)} = \hat{\mathbf{Y}}\mathbf{Y}_s^{(i)}$ ; note that  $\mathbf{Y}_s^{(i)} \in \mathbb{R}^{d^*}$  whereas  $\mathbf{Z}_s^{(i)} \in \mathbb{R}^d$ .
  - 2.4) For each  $j = 1, \dots, d$ , compute  $\hat{\sigma}_{s,j}^{2(i)}$ ,  $\hat{\mu}_{s,j}^{(i)}$  and  $\hat{X}_{s,j}^{(i)}$ , for  $i = 1, \dots, n_{\text{pth}}$  and  $s = t + 1, \dots, t + h$ , via

$$\begin{aligned}\hat{\sigma}_{s,j}^{2(i)} &= \hat{\omega} + \sum_{k=1}^{\hat{p}_{2j}} \hat{\alpha}_{jk} (\hat{X}_{s-k,j}^{(i)} - \hat{\mu}_{s-k,j}^{(i)})^2 + \sum_{l=1}^{\hat{q}_{2j}} \hat{\beta}_{jl} \hat{\sigma}_{s-l,j}^{2(i)}, \\ \hat{\mu}_{s,j}^{(i)} &= \hat{\mu}_j + \sum_{k=1}^{\hat{p}_{1j}} \hat{\phi}_{jk} (\hat{X}_{s-k,j}^{(i)} - \hat{\mu}_j) + \sum_{l=1}^{\hat{q}_{1j}} \hat{\gamma}_{jl} (\hat{X}_{s-l,j}^{(i)} - \hat{\mu}_{s-l,j}^{(i)}), \\ \hat{X}_{s,j}^{(i)} &= \hat{\mu}_{s,j}^{(i)} + \hat{\sigma}_{s,j}^{2(i)} Z_{s,j}^{(i)},\end{aligned}$$

where, for  $s \leq t$ , set  $\hat{X}_{s,j}^{(i)} = X_{s,j}$ ,  $\hat{\sigma}_{s,j}^{2(i)} = \hat{\sigma}_{s,j}^2$ , and  $\hat{\mu}_{s,j}^{(i)} = \hat{\mu}_{s,j}$  for all  $i = 1, \dots, n_{\text{pth}}$ .

- 2.5) Return  $\hat{\mathbf{X}}_s^{(i)} = (\hat{X}_{s,1}^{(i)}, \dots, \hat{X}_{s,d}^{(i)})$ ,  $i = 1, \dots, n_{\text{pth}}$ ,  $s = t + 1, \dots, t + h$ .

Note that Step 2.1) in Algorithm 3.2 can be replaced by sampling from a fitted parametric copula  $\hat{C}_{\text{PM}}$  to obtain the classical approach for sampling paths in the copula–GARCH framework.

While Algorithm 3.2 describes how to simulate paths  $\hat{X}_{n_{\text{pth}},h|\mathcal{F}_t}$  for any simulation horizon  $h$ , we will focus on one-step ahead ( $h = 1$ ) empirical predictive distributions henceforth.

## 3.2 Out-of-sample assessments

We assess two different aspects of out-of-sample performance with data in the test period; again, see Figure 2. We are interested in the following questions. First, how well has the cross-sectional dependence structure been captured? Second, how good are the resulting empirical predictive distributions?

### 3.2.1 Assessing the quality of the cross-sectional dependence model in the test period

We can use the MMD statistic to measure how close the empirical distributions of a fitted GMMN  $\hat{C}_{\text{NN}}$  and a fitted parametric copula  $\hat{C}_{\text{PM}}$  match the cross-sectional dependence structure of the test dataset,  $\mathbf{X}_{\tau+1}, \dots, \mathbf{X}_T$ . This cross-sectional dependence structure can be extracted using the fitted (marginal) ARMA–GARCH models and the fitted PCA model (if dimension reduction is applied), as described in the following algorithm.

**Algorithm 3.3 (Extracting the dependence structure of the test dataset)**

1) Compute  $\hat{\sigma}_{t,j}^2$ ,  $\hat{\mu}_{t,j}$  and  $\hat{Z}_{t,j}$  for  $t = \tau + 1, \dots, T$  and  $j = 1, \dots, d$  via

$$\begin{aligned}\hat{\sigma}_{t,j}^2 &= \hat{\omega} + \sum_{k=1}^{\hat{p}_{2j}} \hat{\alpha}_{jk} (X_{t-k,j} - \hat{\mu}_{t-k,j})^2 + \sum_{l=1}^{\hat{q}_{2j}} \hat{\beta}_{jl} \hat{\sigma}_{t-l,j}^2, \\ \hat{\mu}_{t,j} &= \hat{\mu}_j + \sum_{k=1}^{\hat{p}_{1j}} \hat{\phi}_{jk} (X_{t-k,j} - \hat{\mu}_j) + \sum_{l=1}^{\hat{q}_{1j}} \hat{\gamma}_{jl} (X_{t-l,j} - \hat{\mu}_{t-l,j}), \\ \hat{Z}_{t,j} &= \frac{X_{t,j} - \hat{\mu}_{t,j}}{\hat{\sigma}_{t,j}}.\end{aligned}$$

2) Obtain a sample from the underlying empirical stationary distribution via the transform  $\hat{\mathbf{Y}}_t = \hat{\mathbf{Y}}^\top \hat{\mathbf{Z}}_t$ ,  $t = \tau + 1, \dots, T$ . (Note that  $\hat{\mathbf{Z}}_t \in \mathbb{R}^d$  whereas  $\hat{\mathbf{Y}}_t \in \mathbb{R}^{d^*}$ .)

3) Return the pseudo-observations  $\hat{\mathbf{U}}_t = (\hat{U}_{t,1}, \dots, \hat{U}_{t,d^*})$  of  $\hat{\mathbf{Y}}_t$ , for  $t = \tau + 1, \dots, T$ .

Let  $\hat{U} = (\hat{U}_{\tau+1}^\top, \dots, \hat{U}_T^\top)^\top \in [0, 1]^{(T-\tau) \times d^*}$  denote the pseudo-observations obtained from the test dataset via Algorithm 3.3. Furthermore, let  $U = (\mathbf{U}_1^\top, \dots, \mathbf{U}_{n_{\text{gen}}}^\top)^\top \in [0, 1]^{n_{\text{gen}} \times d^*}$  denote a sample generated from either  $\hat{C}_{\text{NN}}$  or  $\hat{C}_{\text{PM}}$ , where we choose  $n_{\text{gen}} = T - \tau$  (other choices are possible). We can then compute one realization of the MMD statistic  $\text{MMD}(\hat{U}, U; K)$  as in (1). In our analysis in Section 4, we then use an average MMD statistic based on  $n_{\text{rep}}$  repeated samples  $U^{(i)} \in [0, 1]^{n_{\text{gen}} \times d^*}$ ,  $i = 1, \dots, n_{\text{rep}}$ , given by

$$\text{AMMD} = \frac{1}{n_{\text{rep}}} \sum_{i=1}^{n_{\text{rep}}} \text{MMD}(\hat{U}, U^{(i)}; K_{\text{tst}}). \quad (3)$$

**Remark 3.4**

Here, we would like to emphasize that, even though the GMMNs are trained to optimize the MMD statistic on the training dataset, the AMMD metric defined in (3) is still a fair out-of-sample assessment metric since

- 1) it is applied to compare GMMN-generated samples  $U^{(i)}$  against realized innovation copula-samples  $\hat{U}$  from the *test dataset*, not the training dataset; and
- 2)  $K_{\text{tst}} \neq K_{\text{trn}}$ , so a *different* mixture of Gaussian kernels is used for the assessment than the one used for training the GMMN.

**3.2.2 Assessing the quality of empirical predictive distributions**

While there exist numerous metrics to assess univariate or multivariate point forecasts, there are only a handful of metrics that can be used to evaluate the quality of dependent multivariate empirical predictive distributions. We now present two such metrics we will use across all numerical examples.

Firstly, we use a version of the *mean squared error (MSE)* metric defined via the Euclidean norm to assess how well the empirical predictive distribution  $\hat{X}_{n_{\text{pth}},1|\mathcal{F}_{t-1}}$  concentrates around each true value  $\mathbf{X}_t$  in the test dataset, so for  $t = \tau + 1, \dots, T$ . To obtain a single numerical value, we work with an average MSE metric computed over the entire test period  $t = \tau + 1, \dots, T$ , defined by

$$\text{AMSE} = \frac{1}{T - \tau} \sum_{t=\tau+1}^T \frac{1}{n_{\text{pth}}} \sum_{i=1}^{n_{\text{pth}}} \|\hat{\mathbf{X}}_t^{(i)} - \mathbf{X}_t\|_2^2. \quad (4)$$

Secondly, we use the *variogram score* introduced by Scheuerer and Hamill (2015), which, in our context, assesses if the empirical predictive distribution is biased for the distance between any two component samples. For a single numeric summary, we work with an average variogram score (of order  $r$ ) over the entire test period  $t = \tau + 1, \dots, T$ ,

$$\text{AVS}^r = \frac{1}{T - \tau} \sum_{t=\tau+1}^T \sum_{j_1=1}^d \sum_{j_2=1}^d \left( |X_{t,j_1} - X_{t,j_2}|^r - \frac{1}{n_{\text{pth}}} \sum_{i=1}^{n_{\text{pth}}} |\hat{X}_{t,j_1}^{(i)} - \hat{X}_{t,j_2}^{(i)}|^r \right)^2. \quad (5)$$

As numerically demonstrated by Scheuerer and Hamill (2015), by focusing on pairwise distances between component samples, this metric discriminates well between various dependence structures.

## 4 Applications

In this section, we demonstrate the flexibility of our GMMN–GARCH approach when compared to the copula–GARCH approach. To that end, we focus on modeling multivariate yield curve and exchange rate time series.

Before delving into the two financial econometrics applications, we will first detail the selection and setup of component models within our framework that will be utilized for all examples in this section. Specifically, we will describe the choice of marginal time series models, the implementation details for GMMN models, and the choice of parametric copula models used for comparison.

Furthermore, note that all examples considered in this section were implemented in R and can be reproduced using the demo `GMMN_MTS_paper` in the R package `gmn`. In our implementation, the R packages `keras` and `tensorflow` were used as R interfaces to the corresponding namesake Python libraries. All GMMN training was carried out on a single NVIDIA Tesla P100 GPU with 12GB RAM.

### 4.1 Multivariate time series modeling: setup and implementation details

#### 4.1.1 Serial dependence models

For modeling the marginal time series, we take the broad-brush approach and choose to fit ARMA(1,1)–GARCH(1,1) models with scaled  $t$  innovation distributions  $F_j(z_j) = t\nu_j(z_j\sqrt{\nu_j/(\nu_j - 2)})$ ,  $j = 1, \dots, d$ , to each component sample. As mentioned earlier, these models are popular choices for modeling univariate financial time series. To fit them, we use the `fit_ARMA_GARCH(, solver="hybrid")` function from the R package `qrmtools` which relies on the `ugarchfit()` function from the R package `rugarch` (see Ghalanos (2019)).

#### 4.1.2 Cross-sectional dependence models: GMMN architecture and training setup

Taking into consideration that we are working with relatively small number of realizations of time series data in both applications, we find that a single hidden layer architecture ( $L = 1$ ) provides sufficient flexibility. Given the single hidden layer, we experiment with three NN architectures with  $d_1 = 100$  (*GMMN model 1*),  $d_1 = 300$  (*GMMN model 2*) and  $d_1 = 600$  (*GMMN model 3*), respectively, for all examples in this section. We fix  $\phi_1$  to be ReLU since it offers computational efficiency via non-expensive and non-vanishing gradients and  $\phi_2$  to be sigmoid given that our target output lies in  $[0, 1]^{d^*}$ .

As mentioned earlier in Section 2.3.2, we utilize a mixture of Gaussian kernels  $K_{\text{trn}}$  to compute the MMD statistic defined in (1) when training. To this end, we fix  $n_{\text{krn}} = 6$  and choose bandwidth

parameters  $(\sigma_1, \dots, \sigma_6) = (0.001, 0.01, 0.15, 0.25, 0.50, 0.75)$  as done in Hofert, Prasad, et al. (2018). This hyperparameter setting is specifically suited for copula samples or pseudo-observations as they lie in  $[0, 1]^{d^*}$ . Furthermore, it was demonstrated in Hofert, Prasad, et al. (2018) that GMMNs trained with this particular specification of the loss function were capable of learning a wide variety of complex dependence structures.

We choose the dimension of the prior distribution  $F_V$  to be  $p = d^*$ . As a result we obtain a natural  $d^*$ -to- $d^*$  GMMN transform  $f_\theta$ . Following common practice, we select  $\mathbf{V} \sim \mathbf{N}(\mathbf{0}, I_{d^*})$ , where  $I_{d^*}$  denotes the identity matrix in  $\mathbb{R}^{d^* \times d^*}$ . Hence  $\mathbf{V}$  consists of independent standard normal random variables. Since we are working with a modest number of training data points in each of the datasets considered, we opt for a batch optimization procedure presented as a special case ( $n_{\text{bat}} = \tau$ ) of Algorithm 2.1. For the number of epochs, we choose  $n_{\text{epo}} = 1000$  which ensures a sufficiently long training period to obtain accurate results.

### 4.1.3 Cross-sectional dependence models: parametric copulas

For comparison with GMMN–GARCH models, we also present results for a number of different parametric copula models  $C_{\text{PM}}$ . These include Gumbel copulas, normal copulas with exchangeable correlation matrices and  $t$  copulas with exchangeable and with unstructured correlation matrices. We fit these copulas using the maximum pseudo-likelihood method via the function `fitCopula()`, `method="mpl"`) from the R package `copula`. We can generate samples from the fitted copulas using the `rCopula()` function from the same R package. We also produce results for the independence copula which serves as a simple benchmark model.

## 4.2 Yield curve modeling

Analyzing and modeling *zero-coupon bond (ZCB) yield curves*, also referred to as the *term structure of interest rates*, is a critical task in various financial and economic applications. While early research in this area is often solely focused on constructing models of yield curves based on economic theory, the seminal work by Diebold and Li (2006) focused on the critical task of yield curve forecasting.

The primary approach showcased in Diebold and Li (2006) was the embedding of autoregressive models within the parametric structure of the three factor Nelson–Siegel model (Nelson and Siegel 1987) which intuitively characterizes the level, slope and curvature of the yield curve. Since then various approaches for forecasting yield curves have been investigated; see Diebold and Rudebusch (2013) for an overview and Caldeira et al. (2016) for a recently proposed forecast combination approach. Most models proposed and reviewed in the literature are particularly designed towards constructing point forecasts for yield curves. Such point forecasts are typically useful in bond portfolio optimization and in the pricing of certain financial assets. Alternatively, distributional forecasts of ZCB yield curves could potentially be helpful in risk management applications, derivative pricing (via simulation) and economic scenario generation. To that end, in this section, we consider modeling US and Canadian ZCB yield curves using MTS models. We then utilize our fitted GMMN–GARCH models to obtain empirical predictive distributions of these ZCB yield curves.

### 4.2.1 Modeling US and Canadian ZCB data

For US treasury ZCB data, we consider a 30-dimensional yield curve constructed from ZCBs with times to maturity ranging from 1 to 30 years in annual increments. For Canadian ZCB data, we consider a 120-dimensional yield curve constructed from ZCBs with times to maturity ranging from 0.25 to 30 years in quarterly increments. Refer to the R package `qrmdata` for further details about

these data. In particular, we consider these multivariate time series in the time period from 1995-01-01 to 2015-12-31 (2015-08-31 for the Canadian data), treating data from 1995-01-01 to 2014-12-31 as the training set and the remainder as the test dataset.

As a pre-processing step, we begin by applying a simple difference transform to the original time series. We then take the transformed series to be the series  $\mathbf{X}_t$  that we work with.

Following our framework, we first model the marginal time series using the ARMA–GARCH model setup described in Section 4.1.1 with  $\mu_j = 0$ ,  $j = 1, \dots, d$ . Since these data are relatively high-dimensional ( $d = 30$  for the US data and  $d = 120$  for the Canadian data), we apply PCA to the standardized residuals  $\hat{\mathbf{Z}}_t$  for dimension reduction. Yield curves are indeed amenable to good approximations via lower dimensional representations; various dimension reduction techniques such as factor models have been incorporated by various yield curve models (see, e.g., Diebold and Li 2006). We choose the number of top principal components  $k$  to construct the lower dimensional representation for each dataset as follows. We select the smallest  $k \geq 3$  such that the first  $k$  principal components account for at least 95% of the total variance in the standardized residuals  $\hat{\mathbf{Z}}_t$ . For the US data, this choice is  $k = 3$ ; for the Canadian data, it is  $k = 4$ .

### 4.2.2 Assessment

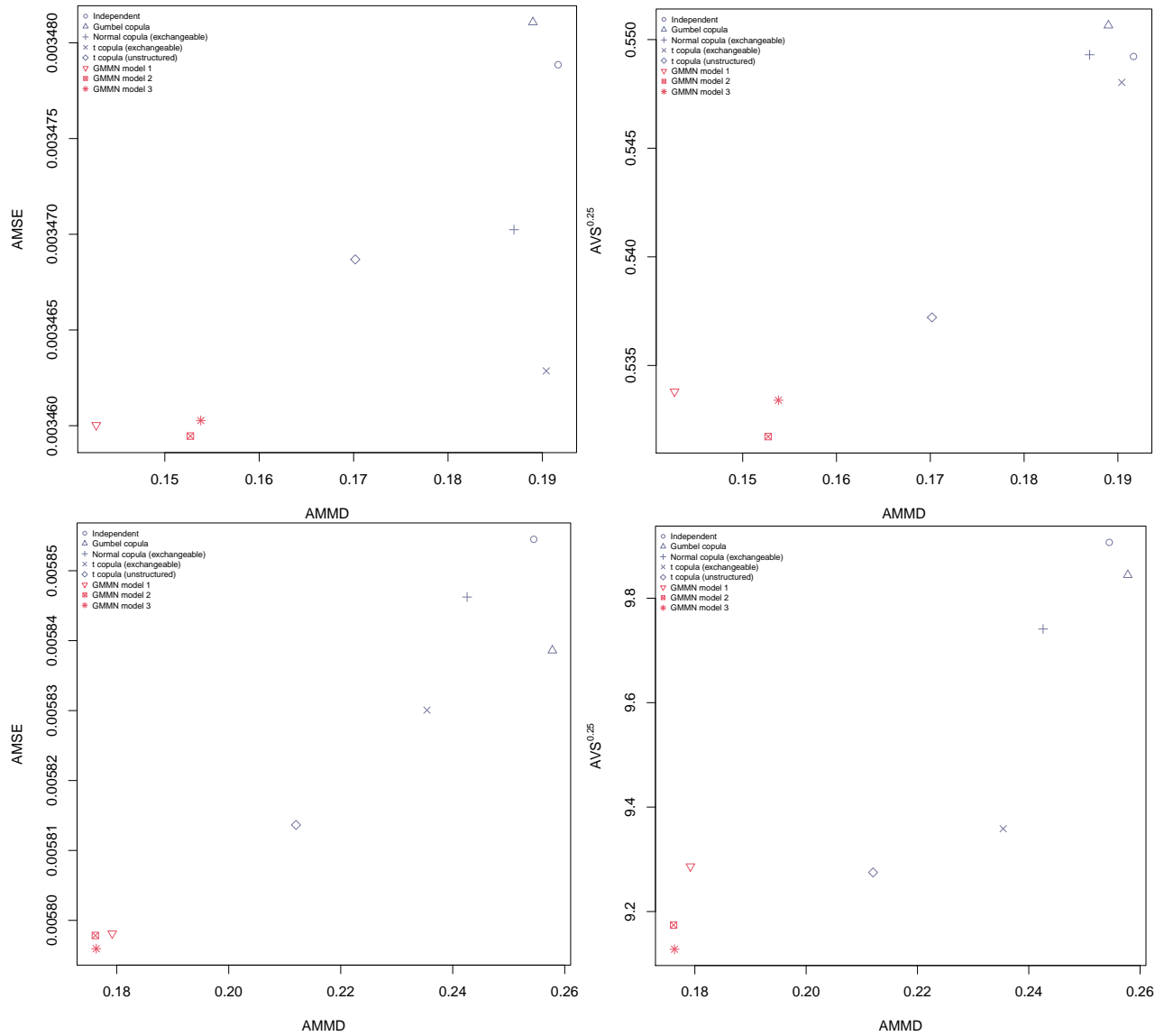
We evaluate the performance of our models on the test dataset using the metrics discussed in Section 3.2. First, we compute the AMMD metric (3) using  $n_{\text{rep}} = 100$  replications to assess the quality of the dependence models in the test period; see the explanations in Remark 3.4 for why the AMMD metric is a fair out-of-sample assessment metric. For the Gaussian mixture kernel  $K_{\text{tst}}$  in (3), we fix  $n_{\text{krn}} = 5$  and select the bandwidth parameters  $\boldsymbol{\sigma} = (0.1, 0.3, 0.5, 0.7, 0.9)$ . Then, to assess if capturing the underlying cross-sectional dependence structure well translates to better one-day-ahead empirical predictive distributions, we compute the AMSE metric (4) and the AVS<sup>r</sup> metric (5) using  $n_{\text{pth}} = 1000$  simulated paths. For the average variogram score metric AVS<sup>r</sup>, a typical choice for the order may be  $r = 0.5$  as stated in Scheuerer and Hamill (2015). However, since their concluding remarks note that smaller values of  $r$  could potentially yield more discriminative metrics when dealing with non-Gaussian data, we choose  $r = 0.25$ .

Figure 3 displays scatter plots of AMSE (left) and AVS<sup>0.25</sup> (right) versus AMMD for the US (top) and Canadian (bottom) data. For both datasets, samples generated from the three GMMN models (see Section 4.1.2) more closely match the underlying cross-sectional dependence structure in their corresponding test datasets than those generated from the four parametric copulas and the independence copula (see Section 4.1.3). Moreover, across the entire spectrum of GMMN–GARCH and copula–GARCH models being studied, it is also clear that better dependence modeling (as measured by the AMMD metric) does indeed translate into better one-day-ahead empirical predictive distributions (as measured by the AMSE and AVS<sup>0.25</sup> metrics). Specifically, all GMMN models clearly outperform the best copula model, i.e., a  $t$ -copula with unstructured correlation matrix, in all three metrics — although among the GMMN models themselves there is not a single best one.

## 4.3 Exchange rate modeling

The modeling and analysis of foreign exchange rate dependence is an important task in risk management applications involving a global portfolio of financial assets. As such, dependent multivariate time series of exchange rates have been previously studied in the copula literature; see, e.g., Patton (2006) or Dias and Embrechts (2010). In this section, we consider modeling foreign exchange rate data with respect to the US dollar (USD) and Pound sterling (GBP) using MTS models. We then utilize our

## 4 Applications



**Figure 3** Model assessments for US (top) and Canadian (bottom) ZCB yield curve data. Scatter plots of AMSE (left) and  $AVS^{0.25}$  (right) computed based on  $n_{pth} = 1000$  simulated paths versus AMMD computed based on  $n_{rep} = 100$  realizations. All models incorporate PCA with  $k = 3$  (US) and  $k = 4$  (Canadian) principal components.

fitted GMMN–GARCH and copula–GARCH models to obtain empirical predictive distributions and Value-at-Risk (VaR) forecasts for portfolios of exchange rate assets.

### 4.3.1 Modeling USD and GBP exchange rate data

For the USD exchange rate data, we consider the daily exchange rates of Canadian dollar (CAD), Pound sterling (GBP), Euro (EUR), Swiss Franc (CHF) and Japanese yen (JPY) with respect to the USD. For the GBP exchange rate data, we consider the daily exchange rates of CAD, USD, EUR, CHF, JPY and the Chinese Yuan (CNY) with respect to the GBP. For further details regarding both the USD and GBP exchange rate data, see the R package `qrmdata`. In particular, we consider these multivariate time series in the time period from 2000-01-01 to 2015-12-31, treating data up to 2014-12-31 as the training set and the remainder as the test dataset. Due to the fixed peg of the CNY against the USD, particularly prior to August 2005, we do not include it in the USD data set.

To begin with, we apply the log-returns transformation to the nominal exchange rates and work with the resulting return series for modeling. Following our framework, we start by modeling the marginal time series using the ARMA–GARCH specification as detailed in Section 4.1.1. Since these datasets are relatively low-dimensional ( $d = 5$  for the USD data and  $d = 6$  for the GBP data), we do not incorporate any dimension reduction step in this analysis.

### 4.3.2 Assessment

Following the setup in Section 4.2.2, we evaluate the performance of our models with the AMMD, AMSE and AVS<sup>0.25</sup> metrics on the test dataset. Figure 4 displays scatter plots of AMSE (left) and AVS<sup>0.25</sup> (right) versus AMMD for the USD (top) and GBP (bottom) data. We can draw the same conclusions from this figure as those from Figure 3. In addition, here we also observe that the independence copula performs noticeably worse than all other models, whether capturing the dependence structure of the innovation distribution or making probabilistic forecasts.

### 4.3.3 Forecasting daily portfolio VaR

As demonstrated in the previous section, GMMN–GARCH models produce better one-day-ahead empirical predictive distributions when compared with various copula–GARCH models. We can utilize these one-day-ahead empirical predictive distributions to extract forecasts of various quantities of interest in risk management. One such popular quantity is the Value-at-Risk (VaR) of a portfolio.

To begin with, consider the portfolio aggregate return  $S_t = \sum_{j=1}^d X_{t,j}$  at time  $t$ . Then, the (theoretical) VaR at confidence level  $\alpha$  and time  $t$  is given by  $\text{VaR}_\alpha(S_t) = F_{S_t}^{-1}(\alpha)$  where  $F_{S_t}^{-1}$  denotes the quantile function of  $S_t$ . In practice, we can compute the empirical  $\alpha$ -quantile of  $S_t$  from its empirical predictive distribution,  $\{\hat{S}_t^{(i)} = \sum_{j=1}^d \hat{X}_{t,j}^{(i)} \mid \mathcal{F}_{t-1}\}_{i=1}^{n_{\text{pth}}}$ . We denote the corresponding forecast by  $\widehat{\text{VaR}}_\alpha(\hat{S}_t)$ . Thus, for each MTS model, we compute daily forecasts  $\widehat{\text{VaR}}_\alpha(\hat{S}_t)$  for every  $t = \tau+1, \dots, T$  in the test period. To assess the quality of these forecasts, we can compute the frequency with which  $S_t$  actually exceeds the daily forecast  $\widehat{\text{VaR}}_\alpha(\hat{S}_t)$  over the entire test period. We expect this frequency to be  $\alpha$ . Hence, we can evaluate our VaR forecasts by measuring the (absolute) error between the actual and the expected exceedance frequency, or simply the *VaR exceedance absolute error*, defined by

$$\text{VEAR}_\alpha = \left| \alpha - \frac{1}{T - \tau} \sum_{t=\tau+1}^T \mathbb{1}_{\{S_t < \widehat{\text{VaR}}_\alpha(\hat{S}_t)\}} \right|. \quad (6)$$



## 4 Applications

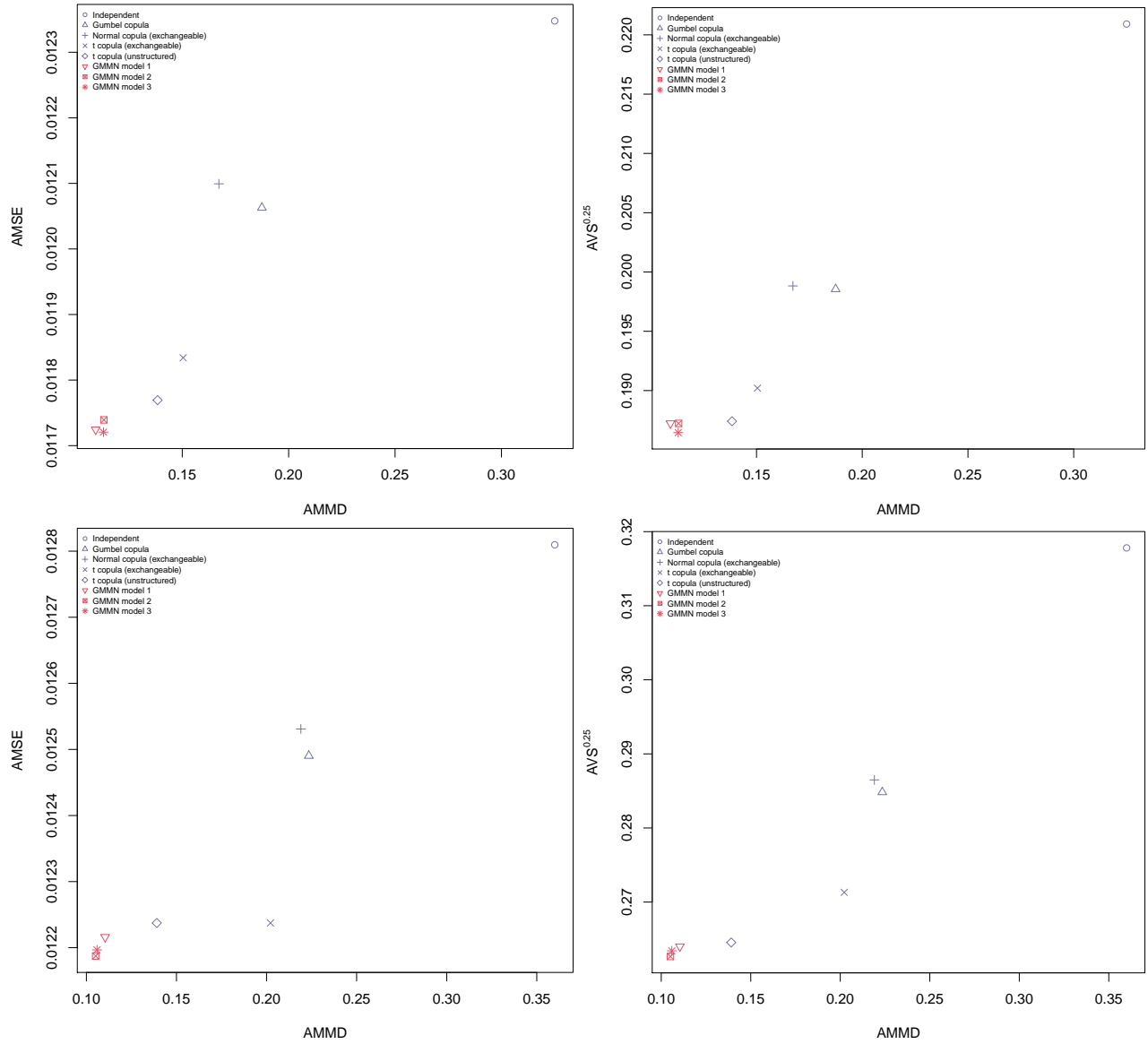


**Figure 4** Model assessments for USD (top) and GBP (bottom) exchange rate data. Scatter plots of AMSE (left) and  $AVS^{0.25}$  (right) computed based on  $n_{pth} = 1000$  simulated paths versus AMMD computed based on  $n_{rep} = 100$  realizations.

## 5 Conclusion

Figure 5 displays scatter plots of  $\text{VEAR}_{0.05}$  versus AMMD for the USD (left) and GBP (right) exchange rates data. For both datasets, the three GMMN–GARCH models produce better daily VaR forecasts of  $\text{VaR}_{0.05}(S_t)$  than the five copula–GARCH models do. Again, there exists a clear general trend that fitted dependence models which more closely match the underlying dependence structures of the test datasets tend to yield better daily forecasts. Particularly, assuming independence amongst the exchange rate returns leads to notably poorer forecasts.

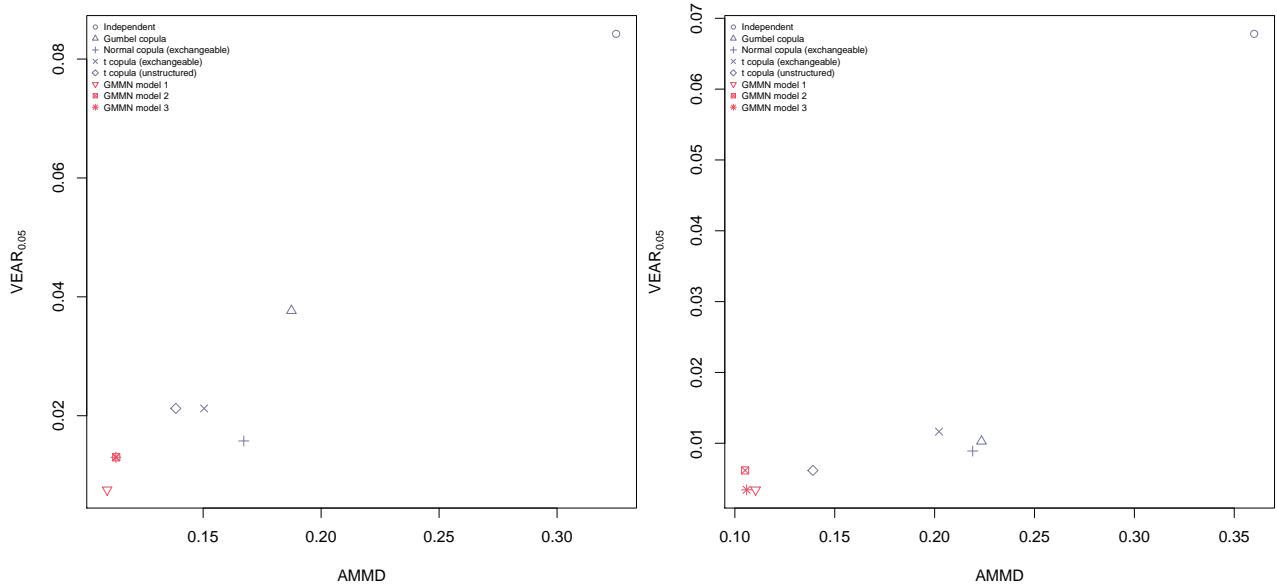


**Figure 5** VaR forecast assessments for USD (left) and GBP (right) exchange rate data. Scatter plots of  $\text{VEAR}_{0.05}$  computed based on  $n_{\text{pth}} = 1000$  simulated paths versus AMMD computed based on  $n_{\text{rep}} = 100$  realizations.

## 5 Conclusion

We introduced generative moment matching networks (GMMNs) for modeling the dependence in MTS data. First, ARMA–GARCH models are used to marginally model serial dependence. Second, for high-dimensional MTS data, a dimension reduction method can be applied. Last, the cross-sectional dependence is modeled by a GMMN. In the popular copula–GARCH approach, the latter step typically requires us to find a parametric copula model which fits the given data well. This can already be a challenging task in moderately large dimensions. By contrast, GMMNs are highly flexible and easy to simulate from, which is a major advantage of our GMMN–GARCH approach. The primary objective of fitting these MTS models is to produce empirical predictive distributions, with which we can then forecast various quantities of interest in risk management such as VaR or expected shortfall.

To showcase the flexibility of our GMMN–GARCH framework, we considered modeling ZCB yield curves and foreign exchange rate returns. Across all the examples considered, we demonstrated that fairly simple GMMNs were able to better capture the underlying cross-sectional dependence than many well-known parametric copulas. Consequentially, we observed that the corresponding GMMN–GARCH models yielded superior one-step ahead empirical predictive distributions. Additionally, for exchange rate data, we demonstrated that GMMN–GARCH models produced more accurate daily portfolio VaR forecasts as well.

For the first two modeling steps in our framework, we used ARMA–GARCH models and principal component analysis. However, a variety of other models can be applied here as long as iid data results as residuals which can then be used to train GMMNs. A potential avenue for future research involves constructing new and highly flexible MTS models by combining different types of marginal time series models and dimension reduction techniques with GMMNs. In particular, one would be interested in capturing different types of (marginal) temporal dependencies and leveraging more sophisticated dimension reduction techniques for constructing even better higher dimensional time series models.

As Hofert, Prasad, et al. (2018) showed, one advantage of GMMNs as dependence models is that one obtains, for free, a quasi-random number generator from the respective model. In how far the low discrepancy property propagates to a variance-reduction effect in forecasted quantities for dependent multivariate time series is also an interesting question of future research.

## References

- Aas, K. (2016), Pair-copula constructions for financial applications: A review, *Econometrics*, 4(4), 43.
- Alexander, C. (2000), A primer on the orthogonal GARCH model, *manuscript ISMA Centre, University of Reading, UK*, 2.
- Almeida, C., Czado, C., and Manner, H. (2016), Modeling high-dimensional time-varying dependence using dynamic D-vine models, *Applied Stochastic Models in Business and Industry*, 32(5), 621–638.
- Bollerslev, T. (1986), Generalized autoregressive conditional heteroskedasticity, *Journal of econometrics*, 31(3), 307–327.
- Bollerslev, T. (1990), Modelling the coherence in short-run nominal exchange rates: a multivariate generalized ARCH model, *Review of Economics and statistics*, 72(3), 498–505.
- Caldeira, J. F., Moura, G. V., and Santos, A. A. P. (2016), Predicting the yield curve using forecast combinations, *Computational Statistics & Data Analysis*, 100, 79–98.
- Dias, A. and Embrechts, P. (2010), Modeling exchange rate dependence dynamics at different time horizons, *Journal of International Money and Finance*, 29(8), 1687–1705.
- Diebold, F. X. and Li, C. (2006), Forecasting the term structure of government bond yields, *Journal of Econometrics*, 130(2), 337–364.
- Diebold, F. X. and Rudebusch, G. D. (2013), *Yield curve modeling and forecasting: the dynamic Nelson-Siegel approach*, Princeton University Press.
- Dziugaite, G. K., Roy, D. M., and Ghahramani, Z. (2015), Training generative neural networks via maximum mean discrepancy optimization, *Proceedings of the Thirty-First Conference on Uncertainty in Artificial Intelligence*, AUAI Press, 258–267, <http://www.auai.org/uai2015/proceedings/papers/230.pdf> (08/24/2019).
- Engle, R. (2002), Dynamic conditional correlation: A simple class of multivariate generalized autoregressive conditional heteroskedasticity models, *Journal of Business & Economic Statistics*, 20(3), 339–350.
- Genest, C. and Segers, J. (2010), On the covariance of the asymptotic empirical copula process, *Journal of Multivariate Analysis*, 101(8), 1837–1845.
- Ghalanos, A. (2019), *rugarch: Univariate GARCH models*. R package version 1.4-1.
- Glorot, X. and Bengio, Y. (2010), Understanding the difficulty of training deep feedforward neural networks, *Proceedings of the thirteenth international conference on artificial intelligence and statistics*, 249–256.
- Gretton, A., Borgwardt, K. M., Rasch, M., Schölkopf, B., and Smola, A. J. (2007), A kernel method for the two-sample-problem, *Advances in neural information processing systems*, 513–520.

## References

- Gretton, A., Borgwardt, K. M., Rasch, M., Schölkopf, B., and Smola, A. J. (2012), A kernel two-sample test, *Journal of Machine Learning Research*, 13(Mar), 723–773.
- Hinton, G. E. and Salakhutdinov, R. R. (2006), Reducing the dimensionality of data with neural networks, *Science*, 313(5786), 504–507.
- Hofert, M., Kojadinovic, I., Maechler, M., and Yan, J. (2018), Elements of Copula Modeling with R, Springer Use R! Series, ISBN 978-3-319-89635-9, doi : 10.1007/978-3-319-89635-9, <http://www.springer.com/de/book/9783319896342> (03/15/2018).
- Hofert, M. and Oldford, R. W. (2018), Visualizing Dependence in High-dimensional Data: An Application to S&P 500 Constituent Data, *Econometrics and Statistics*, 8, 161–183, doi:10.1016/j.ecosta.2017.03.007.
- Hofert, M., Prasad, A., and Zhu, M. (2018), Quasi-Monte Carlo for multivariate distributions via generative neural networks, *arXiv preprint arXiv:1811.00683*.
- Jondeau, E. and Rockinger, M. (2006), The copula–GARCH model of conditional dependencies: An international stock market application, *Journal of International Money and Finance*, 25, 827–853.
- Kingma, D. P. and Ba, J. (2014), Adam: A method for stochastic optimization, <https://arxiv.org/abs/1412.6980> (11/01/2018).
- Li, Y., Swersky, K., and Zemel, R. (2015), Generative moment matching networks, *International Conference on Machine Learning*, 1718–1727.
- McNeil, A. J., Frey, R., and Embrechts, P. (2015), Quantitative Risk Management: Concepts, Techniques, Tools, 2nd ed., Princeton University Press.
- Mercer, J. (1909), Xvi. functions of positive and negative type, and their connection the theory of integral equations, *Philosophical transactions of the royal society of London. Series A, containing papers of a mathematical or physical character*, 209(441-458), 415–446.
- Nelson, C. R. and Siegel, A. F. (1987), Parsimonious modeling of yield curves, *Journal of business*, 473–489.
- Oh, D. H. and Patton, A. J. (2017), Modeling dependence in high dimensions with factor copulas, *Journal of Business & Economic Statistics*, 35(1), 139–154.
- Patton, A. J. (2006), Modelling Asymmetric Exchange Rate Dependence, *International Economic Review*, 47(2), 527–556, [http://public.econ.duke.edu/~ap172/Patton\\_IER\\_2006.pdf](http://public.econ.duke.edu/~ap172/Patton_IER_2006.pdf).
- Patton, A. J. (2012), A review of copula models for economic time series, *Journal of Multivariate Analysis*, 110, 4–18.
- Scheuerer, M. and Hamill, T. M. (2015), Variogram-based proper scoring rules for probabilistic forecasts of multivariate quantities, *Monthly Weather Review*, 143(4), 1321–1334.
- Sklar, A. (1959), Fonctions de répartition à n dimensions et leurs marges, *Publications de L’Institut de Statistique de L’Université de Paris*, 8, 229–231.
- Tse, Y. K. and Tsui, A. K. C. (2002), A multivariate generalized autoregressive conditional heteroscedasticity model with time-varying correlations, *Journal of Business & Economic Statistics*, 20(3), 351–362.